

Chapter 15

Parametric Study on Stainless Steel 316L by Die Sinking EDM for Biomedical Application



Preeti Chauhan, M. A. Saloda, B. P. Nandwana, and S. Jindal

Abstract The electric discharge machine has been acknowledged as a better technique for modification of the surface for biomedical implants. It has many advantages over previously used techniques. Machining by EDM holds many advantages like an increase in wear resistance due to microstructural changes, deposition of oxide and carbide layer over workpiece which enhances the corrosion resistance of material and porosity of material also increases which encourages ingrowth of tissue and transportation of body fluid into it. Increases in surface roughness of elements increase the surface area available for interaction with the bone so higher surface roughness (SR) of biomaterial shows better bone fixation with it than smoother surfaces. In growth of tissues is revealed with higher SR. The parametric study was performed, aiming at increasing the SR of SS 316L for biomedical use and graphite as an electrode was used. Effect of variation in Current (I_d), pulse on time (T_p) and servo voltage (V_d) on SR were studied. Taguchi method was used to evaluate maximum SR. ANOVA was used to identify the most significant factor.

Keywords EDM · Biomedical · Graphite · SS 316L · SR · Taguchi

15.1 Introduction

EDM is used in manufacturing, automotive and aerospace industries for production of complex geometries and finishing of parts [1]. Even nowadays some nonconductive material can also be machined for example zirconia and alumina but it requires coating of conductive material over it to initiate sparking. Once the spark is initiated hydrocarbon oil degenerates into hydrogen and carbon which helps in further sparking and material gets removed. Material from workpiece is removed using thermal energy by erosive effect. It is different from other traditional machining techniques as it does not have physical contact between tool and workpiece which eradicates many problem like chatter, vibration, mechanical stresses which reduces

P. Chauhan (✉) · M. A. Saloda · B. P. Nandwana · S. Jindal
Department of Mechanical Engineering, College of Technology and Engineering, Udaipur,
Rajasthan, India

chances of tool failure [2] and even delicate parts can be easily machined like washing machine agitators. It has wide application in production of mould, dies [3, 4], medical equipment, optical instruments, thin-walled separators in nuclear industry [5] and sports equipment etc. EDM is replacing other traditional machining methods like drilling, grinding, polishing and milling etc. [6]. Figure 15.1 shows important output and input parameters of EDM. Figure 15.2 explains classification of spark erosion machining.

In EDM as shown in Fig. 15.3 replica of tool is formed on workpiece. Material from workpiece is removed using thermal energy produced by sparking between workpiece and tool filled with dielectric fluid between them. EDM is mostly used method for the production of close tolerance shapes, 3D complex shapes. Thermal energy causes the vaporization of material from workpiece and material is removed.

Advantages of EDM machining are:

- Complicated shapes can easily be made by EDM machining.
- Elements with close tolerances can be manufacture by EDM
- Material with any hardness and toughness can be easily machined by EDM.
- As there is no contact between workpiece and tool so material can be machined without any distortion.
- EDM machining is more suitable for delicate material which cannot take stress of traditional machining methods.
- Mirror surface finish can also be obtained by EDM machining by introducing powder additives in dielectric fluid.

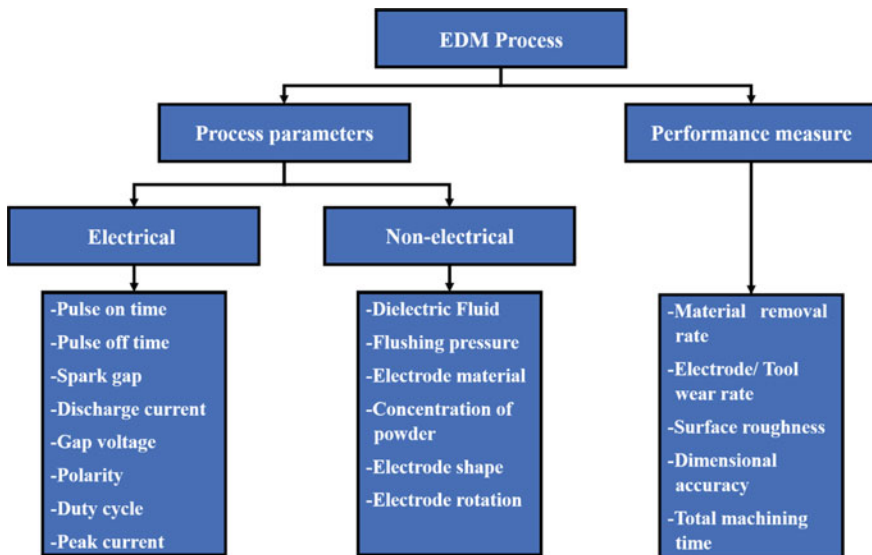


Fig. 15.1 Important output and input parameters for the EDM process [7]

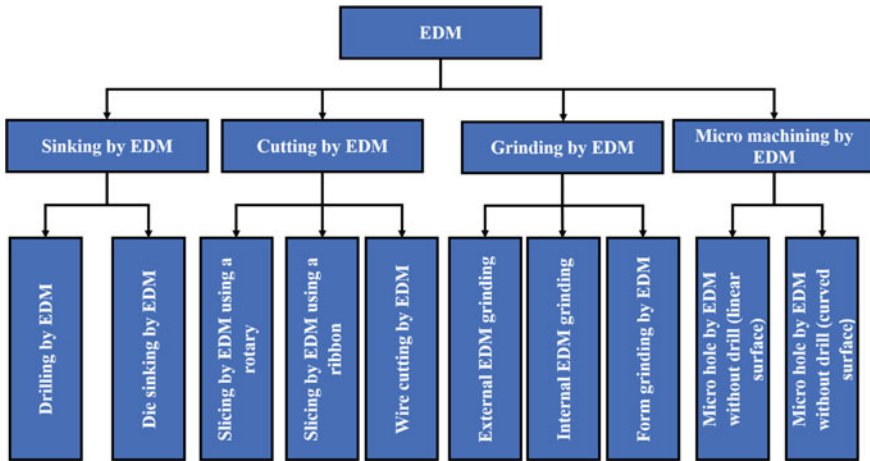


Fig. 15.2 Classification of spark erosion machining [8]

- Due to chip formation in traditional machining methods burs are left on workpiece where as in EDM machining no burs are left on workpiece.

Generally, tool and workpiece are connected with positive and negative polarity respectively where the tool behaves as cathode and workpiece as an anode. Dielectric fluid is an electrically neutral liquid that has some dielectric constant. As the dielectric fluid has some breakdown voltage therefore potential applied between tool and workpiece should be greater than its breakdown voltage otherwise the current will not flow between tool and workpiece. There is RC relaxation circuit in which capacitance gets charged due to the supply of DC power voltage and after that, it gets discharged. When the capacitor discharges its charge between tool and workpiece with minimum resistance. The spark occurs between tool and workpiece which has minimum resistance. There is a minimum resistance between the inter-electrode as there is less gap between these electrodes.

A very large amount of potential is supplied between tool and workpiece when the capacitor gets discharged after charging. An electric field is generated due to electrostatic force which directs electrons from tool towards the workpiece. The electron will move towards workpiece in dielectric fluid when the bond energy of electron is less. Then electron travels with very high velocity and this velocity depends on the potential which is supplied through the capacitor. The electron will move towards the workpiece and collide with the molecules. This collision between electron and molecules generates more positive ions and electrons due to which high concentration of these ions between tool and workpiece within the minimum electrode gap takes place. The positive ion moves in direction of the tool while electrons move towards the workpiece which results in the sparking known as “Plasma Channel”.



Fig. 15.3 ZNC 250 electric discharge machine

The electron collides with the workpiece at a very high velocity. The kinetic energy of these electrons converts into thermal energy which removes the material from the workpiece. This material is removed due to vaporization and melting. The collision of positively charged ions is also responsible for material removal but as their concentration is very less so they result in very less material removal. The plasma channel collapses when the supply of potential between tool and workpiece is stopped. The pressure is generated which removes molten material from the workpiece.

From last few years, to increase MRR, tool is given ultrasonic assisted vibration and tool vibrates, it increases flushing away of debris from workpiece which increases MRR and SR remains unaffected. Rotation of tool also increases the MRR. Some appropriate powder additives in dielectric fluid are being used to improve SR and decreases tool wear. Water as dielectric fluid is being used over other hydrocarbon dielectric fluid for safe environment as decomposition of hydrocarbon oil releases carbon monoxide and methane which is harmful for environment.

15.2 Research Background

Modification of surface for biomaterials is very important for improved surface morphology. There are various techniques available for surface modification like CVD, anodising, PVD and nitriding etc. but due to weak adhesion, bond cannot sustain under repeated loading conditions in corrosive environment and these techniques have become inefficient. Before these techniques coating is required i.e., grit blasting and shot peening which results in increase of production cost [9]. EDM has been recognized for Surface modification of biomaterials in recent years [10]. Elements machined by EDM shows good biocompatibility. Human osteoblast cell reveals better cell proliferation when machined by EDM. EDM machined surface requires no surface preparation as required by other techniques. Corrosion resistance and hardness is improved when machined by EDM which is desirable for biomedical implants. EDM machined samples are preferable substances for MG-63 cells of human osteoblast as per adhesion and growth is concerned [9, 11, 12].

Texture and nature of implant surface defines the behaviour of cells and tissue [13]. More is the surface roughness of elements more is the surface area available for interaction with the bone. Higher surface roughness of biomaterial shows better bone fixation with it and in growth of tissues is revealed with higher surface roughness [13–16]. Main aim of increasing surface roughness is to improve cellular activity. Higher surface roughness obtained by EDM results in deposition of oxide and carbide layers on material which enhances adhesion and ingrowth of bone derived cells [17]. EDM machined surfaces shows improved wear resistance [18, 19]. Porosity of EDM machined surface is increased [20] which enhances the growth of mineralized tissue into pore space which allows body fluid to be transported through interconnected pores [21]. Deposition of oxide and carbide layer after EDM machining results in increase of corrosion resistance and biocompatibility [9]. Table 15.1 explains different types of biomaterials.

SS 316L is mostly used biomaterial as shown in Fig. 15.4 due to low cost, excellent fabrication properties, high fatigue resistance, easy availability, good corrosion resistance, high fracture toughness and good biocompatibility [22–24]. In stainless steel 316L, L stands for low carbon percentage i.e., 0.03%. Table 15.2 shows SS 316L's chemical composition. Graphite was used as tool for machining as shown in Fig. 15.5. Graphite produces more carbide phases on EDM machined surfaces which

Table 15.1 Characteristics of metallic biomaterials (grades ranged from 5 excellent score, to 1, poor score) [27]

| Characteristics | Stainless steel | Co-based alloys | Ti-based alloys |
|----------------------|-----------------|-----------------|-----------------|
| Machinability | | | |
| Conventional | 5 | 1 | 1 |
| Advanced | 5 | 3 | 3 |
| Corrosion resistance | 2 | 3 | 4 |
| Biocompatibility | 1 | 2 | 3 |
| Wear resistance | 2 | 2 | 1 |
| Bioactivity | 1 | 1 | 1 |



Fig. 15.4 Machined workpiece

Table 15.2 Chemical composition of stainless steel 316L [28]

| Elements | | C | Mg | Si | P | S | Cr | Mo | Ni | N |
|---------------|-----|------|-----|------|-------|------|------|-----|------|------|
| Composition % | Min | – | – | – | – | – | 16.0 | 2.0 | 10.0 | – |
| | Max | 0.03 | 2.0 | 0.75 | 0.045 | 0.03 | 18.0 | 3.0 | 14.0 | 0.10 |



Fig. 15.5 Graphite electrode

increases the corrosion resistance of workpiece. Graphite as electrode gives higher surface roughness [25, 26].

Graphite is non-metal which is commonly used in industries as electrode for EDM machining. Graphite has high melting point which makes it more stable than other electrode material. It is comparatively cheaper than other electrodes. It has low density and can be easily machined into desired shape of electrodes. Graphite produces more carbide phases on EDM machined surfaces which increases corrosion resistance of workpiece.

15.3 Research Methods

Whole work was carried out on ZNC-250 Electric Discharge Machine. Schematic diagram of experimental setup is shown in Fig. 15.6. ZNC 250 die sinking EDM was used which has 3 axis x, y and z. Range of x, y and z axis is 250 mm, 250 mm and 200 mm respectively. It has maximum capacity of operating platform of 200 mm. It has maximum processing speed of $200\text{mm}^3/\text{min}$. It consumes maximum power of 6 kW. The machine can hold workpiece of maximum of 200 kg and tool of 25 kg.

SR is a measure of texture of workpiece measured after machining was done. SR is measured by Mitutoyo SURFTTEST SJ-210 as shown in Fig. 15.7. SS 316L was used with dimension $32 \times 32 \times 150$ mm as work piece material. Graphite electrode with dimension $20 \times 20 \times 100$ mm was used as tool.

Surface roughness is measured by contact between Mitutoyo SURFTTEST SJ-210 and workpiece. Technique used here for measuring surface roughness is post process technique and measured by stylus profilometer which has diamond stylus tip. It is moved over machined workpiece and surface roughness is measured. This instrument

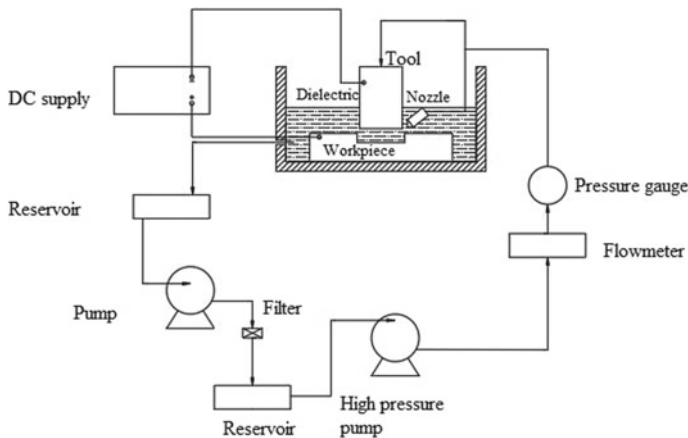


Fig. 15.6 Experimental setup



Fig. 15.7 Mitutoyo SURFTEST SJ-210

uses differential inductance method for detection method. It has measuring range of $360\ \mu\text{m}$ ($-200\ \mu\text{m}$ to $+160\ \mu\text{m}$). Radius of tip is $5\ \mu\text{m}$. Stylus is made of diamond. Radius of skid curvature is $40\ \text{mm}$. Drive range of detector is $21\ \text{mm}$. Its least count is $0.001\ \mu\text{m}$. Bottom configuration has V-shaped trough. The surface roughness is measured by Mitutoyo SURFTEST SJ-210 and data stored in it can be recovered by SPC, Printer or by inserting memory card in it. Here memory card has been used for retrieval of data. Following steps has been performed for insertion of memory card into it and for storing data in it as shown in Fig. 15.8.

In EDM Dielectric fluid use here is Divyol spark erosion oil—25. Machining has to be carried out in absence of oxygen in order to avoid oxidation, when oxidation occurs it leads to poor surface conductivity of workpiece and hinders the further machining of workpiece. That's why dielectric fluid is used as medium to have oxygen free environment for machining. It should have enough sturdy dielectric resistance so that it does not break down easily and while sparking it should be thermally resistant. Most commonly used dielectric fluid are kerosine and deionised water. Tap water can not be used as dielectric fluid as it ionises easily due to presence of salts in it. Dielectric fluid flows over workpiece and tool and removes eroded material from workpiece and helps in further efficient machining of workpiece.

SR has been calculated and examined using Taguchi by Minitab 18. Various steps in Taguchi has been shown in Fig. 15.9. Orthogonal array minimizes number of trials, so it is most effective as it handles number of variables and vast data. Three different parameters i.e., T_p , I_d and V_d are varied and their effect on SR has been studied and design matrix for various parameters are shown in Table 15.3. L9 orthogonal array

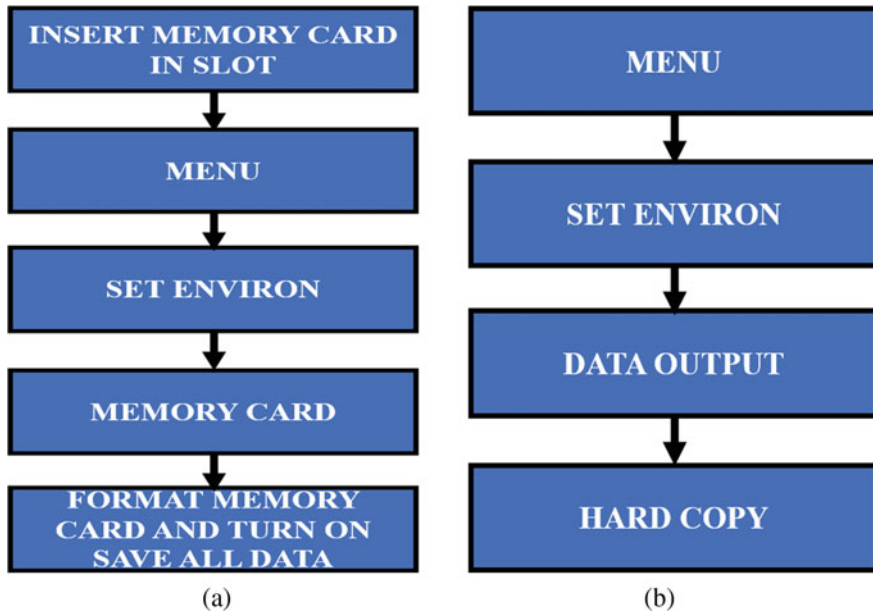


Fig. 15.8 a To insert memory card and b to store data perform following functions in instrument

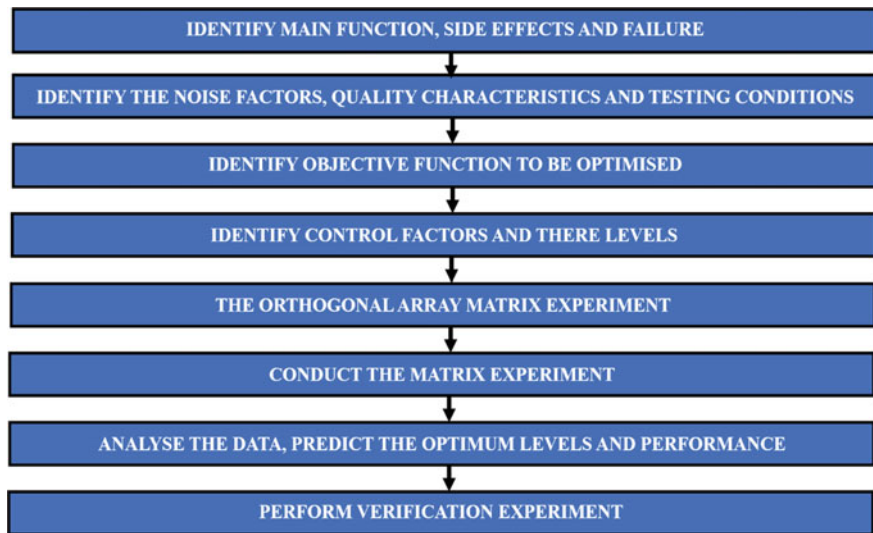


Fig. 15.9 Flow chart for steps in Taguchi design

Table 15.3 Design matrix

| S. No. | I_d | T_p | V_d |
|--------|-------|-------|-------|
| 1 | 10 | 50 | 3 |
| 2 | 10 | 350 | 5 |
| 3 | 10 | 650 | 7 |
| 4 | 14 | 50 | 5 |
| 5 | 14 | 350 | 7 |
| 6 | 14 | 650 | 3 |
| 7 | 18 | 50 | 7 |
| 8 | 18 | 350 | 3 |
| 9 | 18 | 650 | 5 |

was selected for evaluating maximum SR. Larger the better option was selected. ANOVA was used to identify most significant factor.

15.4 Result Discussion

Three parameters T_p , I_d and V_d are varied and their effect has been studied. In this study high range of parameters has been opted as the aim is to increase SR of biomaterial stainless steel 316L for biomedical application. Here T_{off} has been kept constant as with various study it was concluded that T_{off} has very less effect or variation on SR. Here T_{off} taken was 40 μ s. As high range of T_p and I_d has been opted which causes more material removal and more debris, so to provide sufficient time for flushing away of eroded material T_{off} was selected so.

Table 15.4 shows experimental results of machined surface of SS 316L. Larger

Table 15.4 Design matrix

| S. No. | Independent parameters | | | Response | |
|--------|------------------------|------------------|-----------|---------------|-----------|
| | I_d (A) | T_p (μ s) | V_d (V) | SR (μ m) | S/N ratio |
| 1 | 10 | 50 | 3 | 5.752 | 15.1964 |
| 2 | 10 | 350 | 5 | 10.061 | 20.0528 |
| 3 | 10 | 650 | 7 | 11.351 | 21.1007 |
| 4 | 14 | 50 | 5 | 8.055 | 18.1213 |
| 5 | 14 | 350 | 7 | 11.530 | 21.2366 |
| 6 | 14 | 650 | 3 | 13.960 | 22.8977 |
| 7 | 18 | 50 | 7 | 10.501 | 20.4246 |
| 8 | 18 | 350 | 3 | 14.277 | 23.0927 |
| 9 | 18 | 650 | 5 | 18.244 | 25.2224 |

the better option was considered in Taguchi as the aim was to increase SR of material for biomedical use.

Main effect of plot for means graph has been obtained by Taguchi method by software Minitab 18. Main effect plot for means reveals optimization of process parameters at which one can get optimised result for response. Here SR is response and current, pulse on time and servo voltage are factors and for optimization of results higher the better has been chosen. Results of Fig. 15.10 reveals that maximum SR is obtained at combination of parameter I_d 18 A, T_p 650 μ s and V_d 5 V.

Figure 15.11 shows how surface roughness is varied when there is increase in parameters I_d and T_p . Here as we can see in the graph when T_p increases from 50 to 650 μ s for I_d 10 A there is increases in SR. similarly for I_d 14 A and 18 A for increase in T_p SR is increasing. This graph clearly shows that SR increases with increase in I_d and T_p .

In Fig. 15.12 interaction plot is shown between V_d and T_p . Here we can see how graph for SR varies with these two parameters. When V_d increases from 3 to 7 V for T_p 50 μ s there is linear increase in SR. For T_p 350 μ s SR initially decreases then increases for increase in V_d from 3 to 7 V. For T_p 650 μ s SR first increases from 3 to 5 V then it decreases from 5 to 7 V. It is concluded that increase in T_p SR. Whereas for V_d SR increases from 3 to 5 V and then SR decreases from 5 to 7 V.

Figure 15.13 shows interaction plot between I_d and V_d for SR. here for I_d 14 A SR increases for increase in V_d from 3 to 7 V. For I_d 14 A SR initially decreases then increases for V_d from 3 to 7 V. For I_d 18 A, SR increases with increases in value of V_d from 3 to 5 V and there is further decrease in SR with increase in value of V_d from 5 to 7 V. From interaction plots shown above clearly states that SR increases as I_d and T_p increases, whereas with V_d initially SR increases then decreases.

SR plot for 3D surface shown in Figs. 15.14, 15.15 and 15.16 can be seen above. It can be clearly seen that with increase of T_p and I_d , SR. Surface roughness is highly influenced by T_p and then I_d . V_d has very less effect on SR. Only slight change on

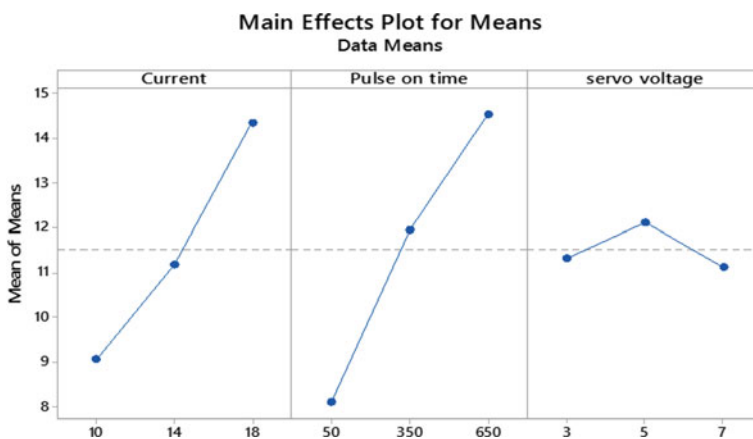


Fig. 15.10 Main effect plot for means of SR

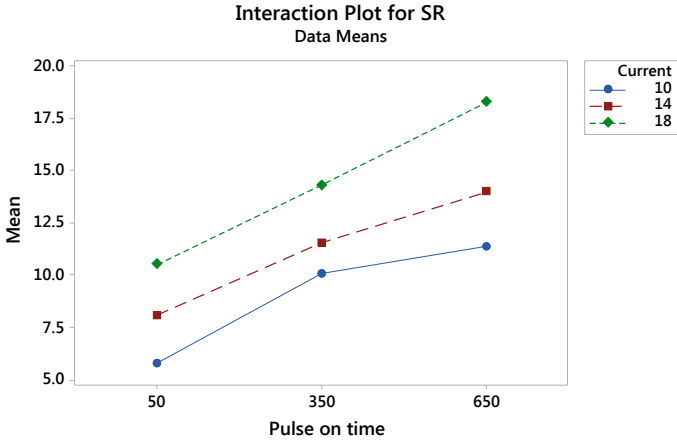


Fig. 15.11 Interaction plot for SR between I_d and T_p

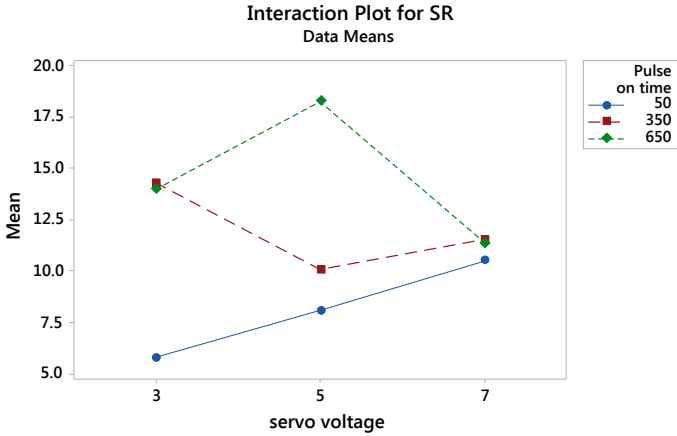


Fig. 15.12 Interaction plot for SR between T_p and V_d

SR can be seen due to change in V_d . From literature survey it was observed that T_p and I_d highly affects SR and increases in value of these parameters increases SR. That's why high value of these parameters was chosen as the main aim of this study was to increase SR which is beneficial for biomedical implants. Maximum surface roughness has been obtained at peak value of T_p 650 μ s, peak value of I_d 18 A and 5 V V_d .

From Table 15.5 it was observed that as T_p and I_d increases SR increases. Increase in V_d results in increase of SR but further increase in V_d leads to decrease of SR.

From Table 15.6, it was observed that T_p and I_d has p value less than 0.05 which shows that these two factors are significant and affects the response i.e. SR. Whereas

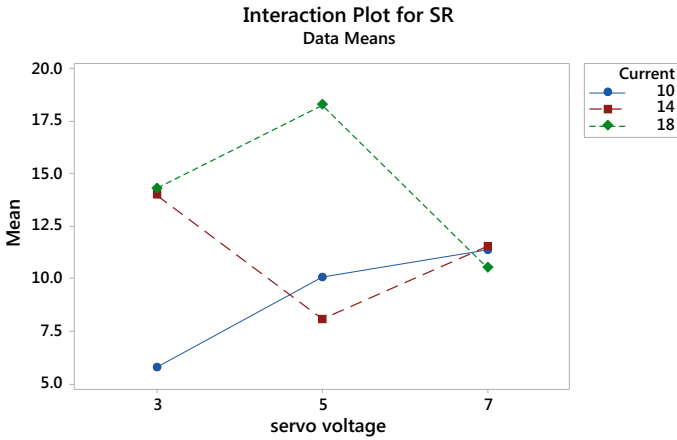
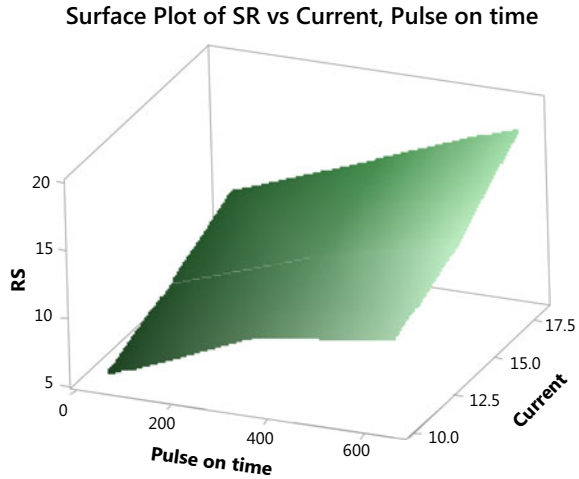


Fig. 15.13 Interaction plot for SR between I_d and V_d

Fig. 15.14 3D surface graph for SR between I_d and T_p



V_d has p value which is greater than 0.05 which shows that V_d is not significant factor and it does effect response much i.e. SR. T_p is most significant factor followed by I_d . V_d has least effect on SR. As I_d increases, supplied energy between tool and workpiece also increases which results in larger crater size of machined workpiece higher is the value of I_d more is the SR. When T_p is increased, supply of energy duration is increased. Hence energy is supplied for longer duration more material is melted and crater size produced is large in size and results in increase of SR. Increase of SR is higher with T_p than I_d . Effect of V_d on SR is not significant as change of V_d has lesser effect on SR.

Fig. 15.15 3D surface graph for SR between I_d and V_d

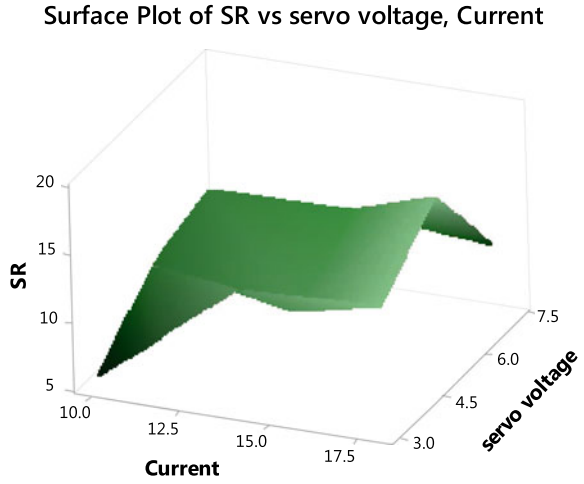


Fig. 15.16 3D surface graph for SR between T_p and V_d

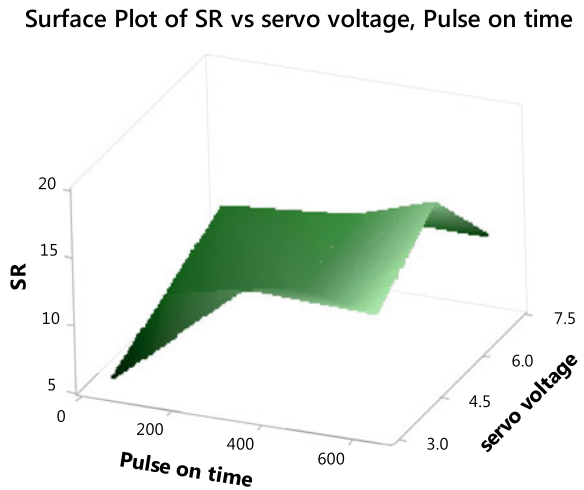


Table 15.5 Rank table for S/N ratio and control machining parameters for SR

| Level | I_d | T_p | V_d |
|-------|-------|-------|-------|
| 1 | 18.78 | 17.91 | 20.40 |
| 2 | 20.75 | 21.46 | 21.13 |
| 3 | 22.91 | 23.07 | 20.92 |
| Delta | 4.13 | 5.16 | 0.74 |
| Rank | 2 | 1 | 3 |

Table 15.6 Rank table for S/N ratio and control machining parameters for SR

| Source | DF | Adj SS | Adj MS | F-Value | P-Value |
|--------|----|---------|---------|---------|---------|
| I_d | 2 | 42.445 | 21.2226 | 74.78 | 0.013 |
| T_p | 2 | 62.575 | 31.2873 | 110.24 | 0.009 |
| V_d | 2 | 1.651 | 0.8255 | 2.91 | 0.256 |
| Error | 2 | 0.568 | 0.2838 | | |
| Total | 8 | 107.238 | | | |

15.5 Conclusion

Following conclusions were drawn from experimental results.

- For SR T_p and I_d are most significant factors. Out of which T_p has more effect on SR than I_d .
- With increases in T_p from 50 to 650 μs SR also increases because as T_p increases energy supplied duration increases which results in crater of larger size on workpiece and hence SR is increased.
- Similarly as I_d increases from 10 to 18 A SR increases. As I_d is increased energy supplied is increased which causes higher temperature and larger crater size and hence SR is increased.
- V_d does not have significant influence over SR, change in V_d has very less effect on SR. As V_d is increased from 3 to 5 V, there is slight increase in SR. As it further increase to 7 V, there is slight decrease in SR.
- Maximum SR 18.244 μm is observed at set of parameters T_p 650 μs , I_d 18 A and V_d 5 V.

References

1. Ho, S.H., Newman, S.T.: State of the art electrical discharge machining (EDM). *Int. J. Mach. Tools Manuf.* **43**, 1287–1300 (2003)
2. Abbas, N.M., Solomon, D.G., Bahari, M.F.: A review on current research trends in electrical discharge machining (EDM). *Int. J. Mach. Tools Manuf.* **47**, 1214–1228 (2007)
3. Barman, S., Vijay, Nagahanumaiah, Puri, A.B.: Surface texture and elemental characterization of high aspect ratio blind micro holes on different materials in micro EDM. *Procedia Mater. Sci.* **6**, 304–309 (2014)
4. Nanimina, A.M., Rani, A.M.A., Ginta, T.L.: Assessment of powder mixed EDM: a review. In: *Proceedings of the 4th International Conference on Production, Energy and Reliability, ICPER (2014)*
5. Volosova, M.A., Okunkova, A.A., Povolotskiy, D.E., Podrabinnik, P.A.: Study of electrical discharge machining for the parts of nuclear industry usage. *Mech. Ind.* **16**, 706 (2015)
6. Pandey, A., Singh, S.: Current research trends in variants of electrical discharge machining: a review. *Int. J. Eng. Sci. Technol.* **2**, 2172–2191 (2010)

7. Ubaid, A.M., Dweiri, F.T., Aghdeab, S.H., Al-Juboori, L.A.: Optimization of electro discharge machining process parameters with fuzzy logic for stainless steel 304 (ASTM A340). *J. Manuf. Sci. Eng.* **140**, 1–13 (2018)
8. Rajesh, R., Anand, M.D.: The optimization of electro discharge machining process using response surface morphology and genetic algorithms. *Procedia Eng.* **38**, 3941–3950 (2012)
9. Prakash, C., Kansa, H.K., Pabla, B.S., Sanjeev, P., Aggarwal, A.: Electric discharge machining—a potential choice for surface modification of metallic implants for orthopedic applications: a review. *J. Eng. Manuf.* **230**, 1–30 (2015)
10. Kumar, V., Beri, N., Kumar, A.: Electric discharge machining of titanium and alloys for biomedical implant applications: a review. *Int. J. Res. Anal. Rev.* **3**, 120–128 (2018)
11. Chauhan, P., Saloda, M.A., Nandwana, B.P., Jindal, S.: Review on research trends in electric discharge machining for biomedical application. *TEST Eng. Manage.* **83**, 2689–2696 (2020)
12. Harchuba, P., Cákóváb, L.B., Stráskýa, J., cákóváb, M.B., Novotná, K., Ceka, M.J.: Surface treatment by electric discharge machining of Ti–6Al–4V alloy for potential application in orthopaedics. *J. Mech. Behav. Biomed. Mater.* **7**, 96–105 (2011)
13. Alla, R.M., Ginjupalli, K., Upadhya, N., Shammas, M., Ravi, R.K., Sekhar, R.: Surface roughness of implants: a review. *Trends Biomater. Artif. Organs* **25**, 112–118 (2011)
14. Saini, M., Singh, Y., Arora, P., Arora, V., Jain, K.: Implant biomaterials: a comprehensive review. *World J. Clin. Cases* **3**, 52–57 (2015)
15. Buser, D., Schenk, R.K., Steinemann, S., Fiorellini, P.P., Fox, C.H., Stich, H.: Influence of surface characteristics on bone integration of titanium implants: a histomorphometric study in miniature pigs. *J. Biomed. Mater. Res.* **25**, 889–902 (1991)
16. Shalabi, M.M., Gortemaker, A., Hof, M.A.V., Jansen, J.A., Creugers, N.H.J.: Implant surface roughness and bone healing: a systematic review. *J. Dent. Res.* **85**, 496–500 (2006)
17. Strasky, J., Janecek, M., and Harchuba, P., 2011. Electric Discharge Machining of Ti-6Al-4V Alloy for Biomedical Use. *WDS'11 Proceedings of Contributed Papers*, 11. 127–131.
18. Shunmugam, M.S., Philip, P.K.: Improvement of wear resistance by EDM with tungsten carbide P/M electrode. *Wear* **171**, 1–5 (1994)
19. Güngör, E., Ekmekçi, B.: Wear resistance of electrical discharge machined surfaces. In: Conference: 3rd International Symposium on Innovative Technologies and Science, At Universidad Politecnica de Valencia, Valencia, Spain, vol. 1, pp. 1080–1089 (2015)
20. Mahamat, A.T.Z., Rani, A.M., Husain, P.: Machining of cemented tungsten carbide using EDM. *J. Appl. Sci.* **11**, 1–7 (2011)
21. Dewidar, M.M., Khalil, K.A., Lim, J.K.: Processing and mechanical properties of porous 316L stainless steel for biomedical applications. *Trans. Nonferrous Met. Soc. China* **17**, 468–473 (2017)
22. Singh, R., Dalhotre, N.B.: Corrosion degradation and prevention by surface modification of biometallic materials. *J. Mater. Sci.* **18**, 725–751 (2007)
23. Simionescu, N., Benea, L.: Corrosion behavior of 316L stainless steel as biomaterial in physiological environment. In: 13th Annual Conference on Materials Science Metal and Manufacturing, Paris, France, November 2017
24. Mariotto, S.F.F., Guido, V., Cho, L.Y., Soares, C.P., Cardoso, K.K.: Porous stainless steel for biomedical applications. *Mater. Res.* **14**, 146–154 (2011)
25. Muttamara, A., Borwornkiatkaew, W., Pronpijit, A., Nuanchom, S.: Effect of graphite electrode to surface's characteristic of EDM. In: MATEC Web of Conferences, vol. 177, pp. 1–4 (2016)
26. Suhardjono: Characteristics of electrode materials on machining performance of tool steel SKD11 with EDM sinking. *ARPN J. Eng. Appl. Sci.* **11**, 986–991 (2016)
27. Aliyu, A.A.A., Abdul-Rani, A.M., Ginta, T.L., Prakash, C., Axinte, E., Razak, M.A., Ali, S.: A review of additive mixed-electric discharge machining current status and future perspectives for surface modification of biomedical implants. *Hindawi Adv. Mater. Sci. Eng.* **2017**, 1–23 (2017)
28. Azom: Stainless Steel Grade 316L Properties, Fabrication and Applications (UNS S31603) (2004). <https://www.azom.com/article.aspx>. Viewed on Nov 2018